Measurement 187 (2022) 110269

Contents lists available at ScienceDirect

Measurement

journal homepage: www.elsevier.com/locate/measurement

An iterative model of the generalized Cauchy process for predicting the remaining useful life of lithium-ion batteries

Guangxu Hong [a], Wanqing Song [a,*], Yan Gao [a], Enrico Zio [b,c], Aleksey Kudreyko [d]

[a] School of Electronic and Electrical Engineering, Shanghai University of Engineering Science, Shanghai, 201620, China
[b] MINES ParisTech, PSL Research University, CRC, Sophia Antipolis, France
[c] Energy Department, Politecnico di Milano, Via La Masa 34/3, Milano 20156, Italy
[d] Department of Medical Physics and Computer Science, Bashkir State Medical University, Lenina st. 3,450008 Ufa, Russia

ARTICLE INFO

Keywords:
Lithium-ion batteries
Remaining useful life
Long-range dependence
Generalized Cauchy iterative model
Predictive maintenance

ABSTRACT

The degradation process of lithium-ion batteries has memory, i.e. it has long-range dependence (LRD). In this paper, an iterative model of the generalized Cauchy (GC) process with LRD characteristics is proposed for the remaining useful life (RUL) prediction of lithium-ion batteries. The GC process uses two independent parameters, fractal dimension and Hurst exponent, to measure the LRD of the degradation process. The diffusion term of the GC iterative model is replaced by the increment of the GC time sequences, constructed via the autocorrelation function (ACF) to describe uncertainty and the LRD characteristics of the lithium-ion batteries capacity degradation. Linear and nonlinear drift terms are used to explain the degradation trend of the lithium-ion batteries capacity. A comparison is made with fractional Brownian motion (FBM) and long-short-term memory (LSTM) network models to show how the GC iterative model has the best performance in RUL prediction of lithium-ion batteries.

1. Introduction

Lithium-ion batteries gradually degrade and age by usage, eventually leading to functional failure [1,2]. RUL prediction is an important task for lithium-ion batteries reliability. It can be based on the estimate of the failure time obtained based on state-of-health monitoring, and can guide predictive maintenance strategies for reducing accident risk [3]. The degradation of lithium-ion batteries is a long-term, slow process [4]. Generally, the capacity in the cycle of charging and discharging is considered as a suitable feature to reflect the degradation trend and, thus, it can be used as health indicator. Then, the RUL of lithium-ion batteries can be defined with respect to a minimum capacity threshold level, typically 20–30% of the rated capacity [5]. In this way, the RUL prediction problem is transformed into a capacity prediction problem with reference to the preset failure threshold (FT).

The existing RUL prediction methods for lithium-ion batteries can be mainly divided into three categories: filtering methods, artificial intelligence methods and stochastic process methods. Wang et al. [6] developed a degradation method based on a spherical particle filter to achieve RUL prediction of lithium-ion batteries. Zheng and Fang [7,8] proposed a hybrid prediction model based on unscented Kalman filter to achieve RUL prediction of lithium-ion batteries. Other developments of filtering methods, such as particle filter and Kalman filter, can be found in [9-11]. Filtering methods have obvious advantages under certain application conditions [12], but there are also three main disadvantages that hinder the feasibility of their use in practical applications of lithium-ion batteries RUL prediction: in general, the prediction accuracy of filtering methods is susceptible to ambient temperature and time-varying current [13]; particle filtering methods suffer the problem of particle paucity due to resampling [14]; particle filtering methods may have difficulties in determining the key parameters to describe the process of lithium-ion battery capacity degradation [15]. Zhang et al. [2] developed a RUL prediction method based on LSTM recurrent neural network. Chen et al. [16] proposed a prediction model based on empirical mode decomposition and deep recurrent neural network to show the LSTM can give good prediction accuracy. Nuhic et al. [17]

Abbreviations: LRD, long-range dependence; GC, generalized Cauchy; RUL, remaining useful life; ACF, autocorrelation function; FBM, fractional Brownian motion; LSTM, long-short-term memory; FT, failure threshold; MLE, maximum likelihood estimation; PDF, probability density function; RS, rescaled range; FPT, first prediction time; EOL, end-of-life; MAE, mean absolute error; RMSE, root mean square error; HD, health degree.

* Corresponding author.
E-mail address: swqls@126.com (W. Song).

https://doi.org/10.1016/j.measurement.2021.110269
Received 30 May 2021; Received in revised form 18 September 2021; Accepted 30 September 2021
Available online 27 October 2021

proposed a method based on support vector machines to predict the RUL of lithium-ion batteries. Li et al. [18] developed a least squares support vector machine model, based on data-driven and model fusion, to predict the RUL of lithium-ion batteries. Li et al. [19] proposed an Elman neural network model to predict the RUL of lithium-ion batteries. The disadvantages of artificial intelligence methods are that mainly the expected value of the RUL can be obtained, whereas the uncertainty in the prediction can be achieved only at the expense of large computational efforts [13]. In addition, the artificial intelligence methods require large-scale training data and overtraining can cause the problem of falling in a local optimum [20]. The stochastic process methods for RUL prediction have good characteristics, useful also for characterizing the uncertainty in the prediction of the degradation process of lithium-ion batteries. These methods perform the RUL prediction based on probability theory and the development of a stochastic model. The stochastic model can flexibly reflect the uncertainty of the degradation process [21]. For this reason, they are finding applications in lithium-ion batteries RUL prediction [22], e.g. based on Markov process and Wiener process [22,23].

Since the degradation of lithium-ion batteries is a continuous and slow process, it has LRD characteristics [24]. However, modeling based on Wiener process relies on the Markov hypothesis [21], and the incremental independence of the Wiener process cannot reflect the LRD characteristics of the lithium-ion batteries degradation process. To overcome this limitation, in this paper we propose a GC iterative model with LRD characteristics to predict the RUL of lithium-ion batteries.

Li defined a GC process with LRD characteristics and associated uncertainty to describe fractal time sequences [25]. The LRD characteristic of the GC process is evaluated by its ACF, which is composed of the fractal dimension D and the Hurst exponent H [26]. If the ACF integral $\int_{-\infty}^{+\infty} R(\tau)d\tau = \infty$ of the GC process diverges, the GC process is considered to have LRD characteristics [27]. The GC process satisfies LRD, which means that its ACF slowly decays to the extent of integral divergence, so that the correlation between two different points that are far apart in time cannot be ignored. Based on the integration of the above-mentioned ACF, Lim and Li obtained that the GC process satisfies the LRD characteristic when $0 < (4-2D)(2-2H) \leq 1$ [27]. Therefore, the LRD characteristics are jointly described by the Hurst exponent H and the fractal dimension D, and the GC time sequences are randomly generated considering the ACF of the GC, which captures the uncertainty in the process [25]. Therefore, the GC iterative model not only overcomes the problem of accounting for the LRD characteristics of the lithium-ion batteries degradation process, which the Markov process and the Wiener process cannot, but also overcomes the problem of representing the uncertainty in the prediction, which cannot be inexpensively achieved by the artificial intelligence methods. The FBM model is another model with LRD characteristics, which can be used to predict the RUL of lithium-ion batteries [24]. However, there is a linear relationship $H+D=2$ between H and D, so that only one parameter can be used to describe the LRD characteristics. When $0.5 < H < 1$, the FBM has LRD characteristics [24]. Compared with the FBM model, the superiority of the GC iterative model lies in the availability of the two parameters H and D, which are independent of each other: this makes the GC iterative model more flexible than FBM to describe the LRD characteristics.

In this paper, linear and nonlinear drift terms (such as a power function drift term) are used to describe the degradation trend of lithium-ion batteries. In addition, the diffusion term of the GC iteration model is replaced by the increment of the GC time sequences to solve the problem of the uncertainty and LRD characteristic prediction of the lithium-ion batteries degradation process. Then, the parameters of the GC iterative model are obtained by the maximum likelihood estimation (MLE) method. The first arrival time of the lithium-ion batteries RUL can be obtained by evaluating when capacity exceeds the preset FT. Furthermore, the probability density function (PDF) of the RUL can be obtained by Monte Carlo simulation [28,29]. Finally, real data of lithium-ion battery capacities are used to verify the feasibility of the GC iterative model, and a comparison is made with FBM and LSTM.

The organization of this paper is as follows. The LRD characteristics of the GC process are briefly discussed in Section 2. In Section 3, we describe the iterative model based on the GC process and the procedure for estimating the parameters of the iterative model. In Section 4, the lithium-ion batteries RUL is predicted by the GC iterative model, and a comparison is made with the FBM and LSTM models. Finally, the conclusion of this paper is given in Section 5.

2. The LRD characteristics of the generalized Cauchy process

To analyze the LRD characteristics of the GC process, it is essential to introduce the ACF. Li et al. [25] gave the definition of ACF for the GC process:

$$r_y(\tau) = E[y(t+\tau)y(t)] = (1+\tau^{\alpha})^{-\beta/\alpha} \tag{1}$$

where $\tau > 0, \beta > 0$, $0 < \alpha \leq 2$, and $y(t)$ is GC process. When $\alpha = 2$ and $\beta = 2$, the GC process degenerates into a classical Cauchy process.

In the GC process, the LRD characteristics are described by parameters D and H, which reflect the local and global properties, respectively. The parameter α can be described by the fractal dimension D, which is a measure for roughness, and the parameter β can be described by the Hurst exponent H, which is a measure of self-similarity. The specific relationships are $\beta = 2-2H, \alpha = 4-2D$ [27].

If the ACF of a stochastic process $y(t)$ satisfies $\int_0^{+\infty} r_y(\tau)d\tau = \infty$, it is said that the stochastic process satisfies LRD. According to the definition of LRD, we obtain that when $0 < \alpha\beta \leq 1$, the GC process satisfies the LRD condition [27]:

$$\int_0^{+\infty} r_y(\tau)d\tau = \int_0^{+\infty} (1+\tau^{\alpha})^{-\beta/\alpha}d\tau = \infty \quad if \;\; 0 < \alpha\beta \leq 1 \tag{2}$$

That the GC process satisfies LRD means that its ACF slowly decays to the extent of integral divergence, so that the correlation between two different points that are far apart in time cannot be ignored. When $0 < \alpha\beta \leq 1$, the range of Hurst exponent values is $0 < (4-2D)(2-2H) \leq 1$. The ACF with two parameters is described in Fig. 1. It is shown that the ACF curve has not yet decayed to zero after a long time under LRD condition: the high H and low D values contribute to the slow decay of the ACF curve, until the integral of the ACF in Eq. (2) diverges.

Next, the LRD characteristics are explained from the perspective of PDF. Carrillo et al. gave the PDF of the GC process [30]:

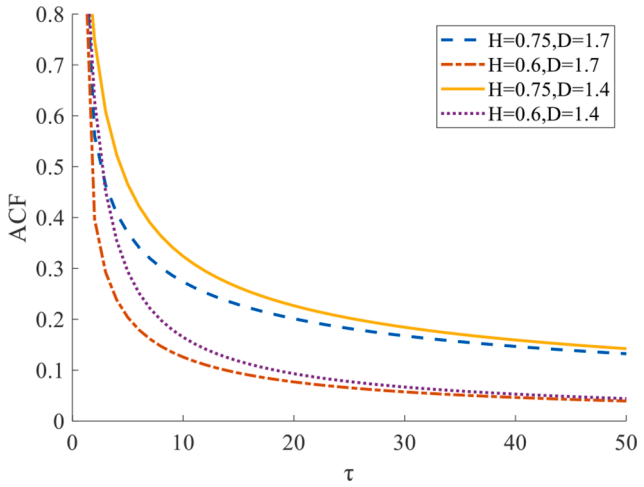

Fig. 1. The ACF of the GC process.

$$f_{GC}(y) = \frac{\rho\Gamma(2/\rho)\gamma}{2\left(\Gamma(1/\rho)\right)^2}(\gamma^\rho + |y-u|^\rho)^{-2/\rho} \tag{3}$$

where u is position parameter, the γ is range parameter, the ρ is heavy-tailed parameter. $\Gamma(\cdot)$ represents the gamma function. In Fig. 2, the influence of the parameters of the GC process on the PDF is shown.

The range parameter u is the symmetry axis of the PDF. The range parameter γ indicates the discrete degree of the PDF. The smaller the range parameter, the more concentrated the value of the points in the PDF. The heavy-tailed parameter ρ indicates the heavy tailed degree of the PDF. The smaller the heavy-tailed parameter, the heavier the tail of the PDF. The GC process is a heavy-tailed distribution when $0 < \rho \leq 2$. From Taqqu's law [30], we can obtain that the stochastic process $x(t)$ exhibits a heavy-tail in the PDF, which is equivalent to the LRD characteristics in the ACF. In fact, the ACF of the GC process can be written as $r_y(t_1,t_2) = E[y(t_1)y(t_2)] = \iint y(t_1)y(t_2)f_{GC}(y;t_1,t_2)dy(t_1)dy(t_2)$, according to Eq. (1): therefore, the slow decay of the PDF leads to the slow decay of the ACF.

3. Iterative model

3.1. Iterative model based on generalized Cauchy process

Since the degradation of lithium-ion batteries is a continuous and slow process, it has LRD characteristics. In this paper, we use the GC-driven diffusion term to describe the uncertainty and LRD characteristics of the degradation process of lithium-ion batteries. Similarly to the stochastic differential equation of Wiener process and FBM, the stochastic differential equation of the GC iterative model is written as [31,32]:

$$dX(t) = \lambda\varphi(t)dt + \sigma(t)dGC(t) \tag{4}$$

where $X(t)$ is the degradation process of lithium-ion batteries capacity. The $\lambda\varphi(t)$ is the drift term, reflecting the degradation trend. The $\sigma(t)dGC(t)$ is the diffusion term, reflecting the degradation uncertainty and LRD characteristics. In this paper, the linear drift term λ and nonlinear drift term (such as a power function drift term λt^b) are used to reveal the degradation trend of lithium-ion batteries. We bring the drift term and the simplified diffusion term σ into Eq. (4) to obtain Eqs. (5) and (6):

$$M1: dX(t) = \lambda dt + \sigma dGC(t) \tag{5}$$

$$M2: dX(t) = \lambda t^b dt + \sigma dGC(t) \tag{6}$$

where $dGC(t)$ is the increment of the GC time sequences. In Figs. 3 and 4,

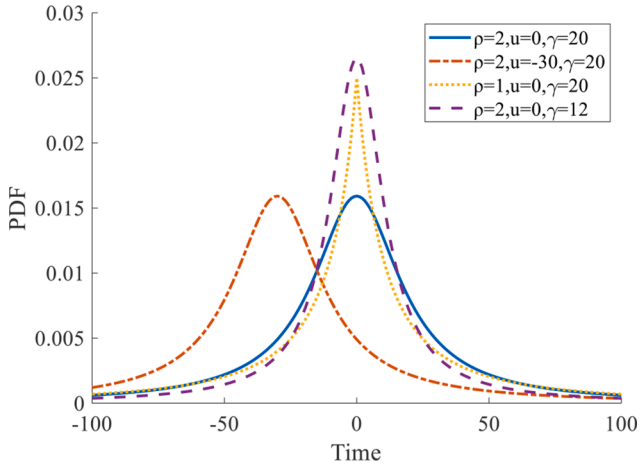

Fig. 2. PDF of the GC process.

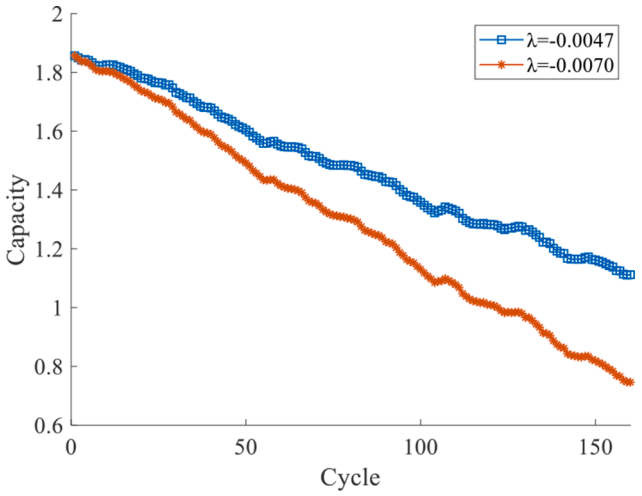

Fig. 3. Linear degradation trend.

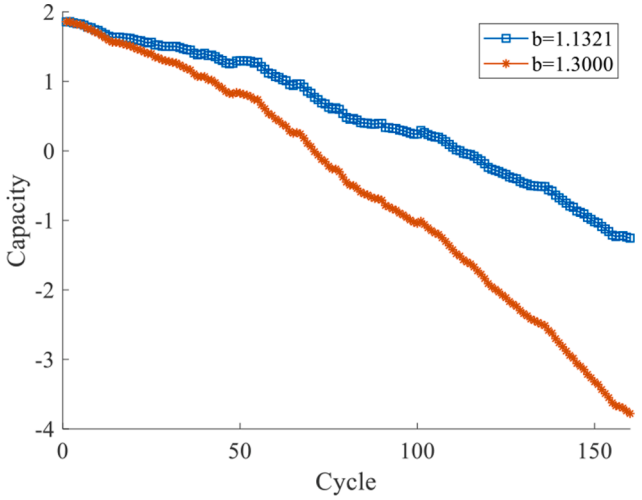

Fig. 4. Power function degeneration trend.

the linear and power function degradation trends under different parameters are simulated, respectively.

where $\lambda > 0$ indicates the upward degradation trend, $\lambda < 0$ indicates the downward degradation trend, and the value of λ reflects the degradation speed. The larger the λ, the faster the degradation speed. The parameter b reflects the speed at which the power function degenerates. The larger the value of b, the faster the degradation speed.

The specific construction steps of the increment of the GC time sequence are as follows.

Step 1: The power spectrum $S(\omega)$ is the Fourier transform of the ACF.

$$S(\omega) = F\left[\left(1+|\tau|^\alpha\right)^{-\beta/\alpha}\right] \tag{7}$$

Let $h(t)$ be the impulse response and $H(\omega)$ be the Fourier transform of $h(t)$. We have the relationship $S(\omega) = |H(\omega)|^2$, between $S(\omega)$ and $H(\omega)$. According to the relationship between the impulse response $h(t)$ and the power spectrum $S(\omega)$, we put Eq. (7) into Eq. (8) to obtain:

$$h(t) = F^{-1}\left[\sqrt{S(\omega)}\right] = F^{-1}\left\{F\left[\left(1+|\tau|^\alpha\right)^{-\beta/\alpha}\right]^{0.5}\right\} \tag{8}$$

Step 2: The GC time sequence can be constructed by convolution of the white noise and impulse response. According to the relationships $\beta = 2-2H, \alpha = 4-2D$, the specific expression is [25]:

$$GC(t) = w(t)*h(t) = w(t)*F^{-1}\left\{F\left[\left(1+|\tau|^{4-2D}\right)^{-\frac{\lambda-2H}{4-2D}}\right]^{0.5}\right\} \tag{9}$$

where $w(t)$ is the Gaussian white noise time sequence, the symbol * represents convolution.

Step 3: Set the time interval and construct the difference $dGC(t) = GC(t+1) - GC(t)$ of the time sequences to obtain the increment according to Eq. (9). Based on the above GC time sequence construction steps, the specific flowchart is shown in Fig. 5.

In Fig. 6, the GC time sequence is generated with $H = 0.6$ and $D = 1.4$, and the corresponding GC incremental time sequence is shown in Fig. 7.

3.2. Parameter estimation of the iterative model

In Eqs. (5) and (6), five unknown parameters need to be estimated, i.e., H, D, λ, σ and b. These unknown parameters are recorded as $\Phi = [H, D, \lambda, \sigma, b]^T$. The parameters H and D in the ACF of the GC process are not coupled with the parameters λ, σ, and b, and thus can be estimated separately. The Hurst exponent H is estimated by the rescaled range (RS) method [33], and the fractal dimension D is estimated by the box dimension method [33]. The nonlinearity of the power law drift term makes it hard to obtain a specific solution of b. We solve this problem through the Nelder-Mead simplex algorithm [34]. Eventually, we use the MLE method to estimate the parameters λ and σ. The specific steps for parameter estimation are as follows.

Step 1: Obtain the estimated value $\widehat{H}$ of the Hurst exponent H by the RS method [33].

$$\frac{R}{S} = \frac{\max\limits_{1\le i\le N} X_{i,N} - \min\limits_{1\le i\le N} X_{i,N}}{\sqrt{\frac{1}{N-1}\sum\limits_{i=1}^{N}(X_i - \langle X\rangle)^2}} \tag{10}$$

where $\langle X\rangle$ is the mean of the degradation process of lithium-ion batteries capacity, X_i and $X_{i,N}$ are deviations. R is range and S is standard deviation. According to the logarithmic relationship between N and R/S, the estimated value of H is obtained from the following equation:

$$\ln\frac{R}{S} = H\ln N + C \tag{11}$$

where C is a constant. The estimated value $\widehat{H}$ of Hurst exponent H is the slope of the least square fitting of N and R/S in logarithmic coordinates.

Step 2: Calculate the estimated value $\widehat{D}$ of the fractal dimension D by the box dimension method [33]:

$$\widehat{D} = \lim_{l\to 0}\frac{\ln(N_l)}{\ln(1/l)} \tag{12}$$

where l is the side length of the squares and N_l is the total number of squares occupied by the degradation process of lithium-ion batteries capacity.

Step 3: Take the estimated values of $\widehat{H}$ and $\widehat{D}$ into the LRD evaluation: if $0 < (4-2D)(2-2H) \le 1$ is not satisfied, the GC iterative model cannot be used to predict the RUL of the lithium-ion batteries; if it is satisfied, the $\widehat{H}$ and $\widehat{D}$ are put into Eq. (9) to generate the GC time sequences.

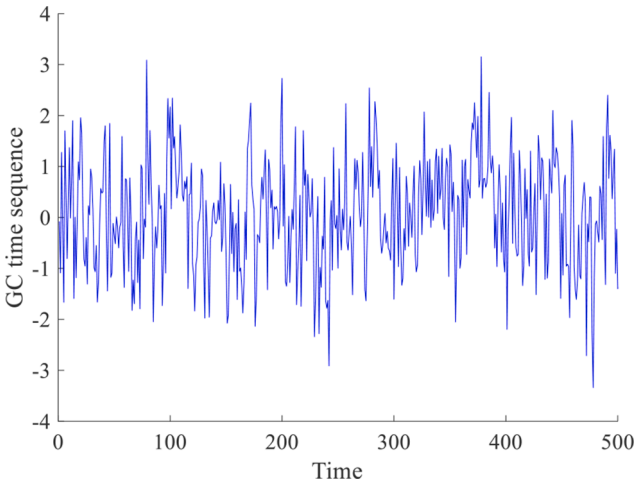

Fig. 6. GC time sequence.

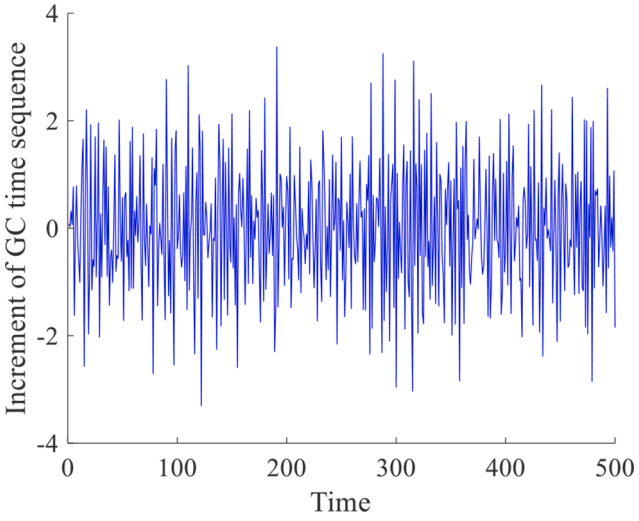

Fig. 7. Increment of GC time sequence.

Step 4: Use the MLE method to obtain the estimated values $\widehat{\lambda}$ and $\widehat{\sigma}$. The observed values of the degradation process at ordered times $t_0, t_1, \cdots, t_n$ are denoted as $X = [X_0, X_1, \cdots, X_n]^T$. Let $\theta = [\varphi'(t_1), \varphi'(t_2), \cdots, \varphi'(t_n)]^T$. Suppose that the increment of the GC process follows a normal distribution. According to the independent property of the GC increment, $x = [X_1 - X_0, X_2 - X_1, \cdots, X_n - X_{n-1}]^T$ is a multi-dimensional normal distribution, and follows a normal distribution $x\ N(\lambda\theta, \sigma^2 Cov)$. Cov is the covariance matrix of the GC process. According to the joint PDF of the multi-dimensional normal distribution [24], the likelihood function is obtained as follows:

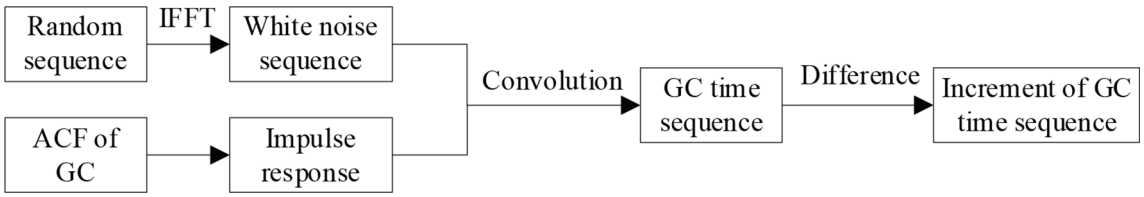

Fig. 5. Flowchart of the procedure for generating the incremental time sequences.

$$g(x) = \left(2\pi\sigma^2\right)^{-\frac{n}{2}}|Cov|^{-\frac{1}{2}}exp\left[-\frac{1}{2\sigma^2}(x-\lambda\theta)^T Cov^{-1}(x-\theta T)\right] \tag{13}$$

Take the logarithm of Eq. (13) to obtain Eq. (14):

$$\ln(g) = -\frac{n}{2}\ln\left(2\pi\sigma^2\right) - \frac{1}{2}\ln|Cov| - \frac{1}{2\sigma^2}(x-\lambda\theta)^T Cov^{-1}(x-\lambda\theta) \tag{14}$$

Calculate the partial derivatives of equation (14) with respect to λ and σ^2, and set the partial derivatives to zero to obtain the estimated values $\widehat{\lambda}$ and $\widehat{\sigma}$, respectively:

$$\widehat{\lambda} = \frac{\theta^T Cov^{-1}x}{\theta^T Cov^{-1}\theta} \tag{15}$$

$$\widehat{\sigma} = \sqrt{\frac{1}{N}(x-\lambda\theta)^T Cov^{-1}(x-\lambda\theta)} \tag{16}$$

Step 5: Use Nelder-Mead simplex algorithm and fminsearch function in MATLAB to obtain the estimated value $\widehat{b}$.

Step 6: Take the results of parameter estimation into Eqs. (5) and (6). The specific flowchart of parameter estimation procedure is shown in Fig. 8.

3.3. Remaining useful life prediction

The aim is to predict the RUL of the lithium-ion batteries by developing a GC iterative model. The first prediction time (FPT) is the starting point of the prediction. Generally, lithium-ion batteries functional failure occurs when the capacity exceeds the FT for the first time, which is called end-of-life (EOL). The relationship between RUL, EOL, and FPT is shown schematically in Fig. 9. Some jump points on the capacity degradation of lithium-ion batteries are described by the fluctuations of the GC time sequence with LRD characteristics. The degradation process of lithium-ion batteries capacity reaches the FT for the first time as [35]:

$$T_{EOL} = \inf\{T_{EOL} : X(T_{EOL}) \geq w_0 | X(0) < w_0\} \tag{17}$$

where w_0 is the given FT, T_{EOL} represents the moment when the fault threshold w_0 is reached for the first time, *inf* is the infimum, $X(t)$ is the degradation process of lithium-ion batteries capacity.

When the starting point of prediction does not satisfy $t = 0$, the RUL is defined as [29,35]:

$$RUL = \inf\{RUL : X(t + RUL) \geq w_0 | X(t) < w_0\} \tag{18}$$

where t is the FPT, RUL is the predicted RUL. In the RUL prediction of lithium-ion batteries, RUL is represented by the number of cycles of charge and discharge. The predicted RUL can be obtained by the GC iterative model and the equation (18). The RUL prediction schematics is presented in Fig. 9.

The generated GC time sequences is not deterministic and the actual RUL cannot be accurately reflected by few estimated values of RUL. To consider the prediction uncertainty in the RUL, we use Monte Carlo simulation to generate RUL values for obtaining the PDF of the RUL. We, then, take the most probable value of the RUL (corresponding to the maximum value of PDF) as point value.

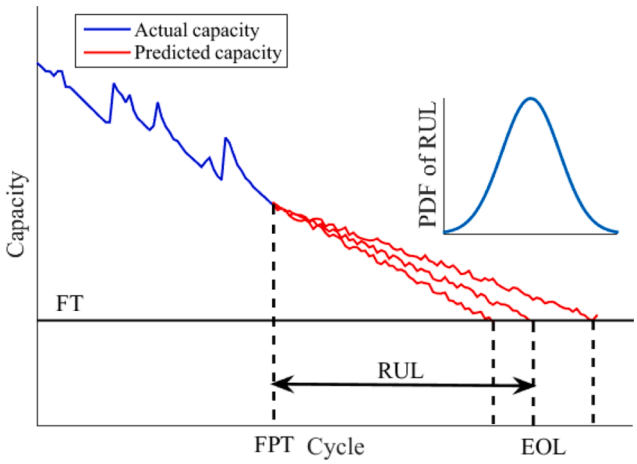

Fig. 9. RUL prediction schematics.

4. Case study

We consider the lithium-ion batteries capacity data from NASA Ames database to verify the feasibility of the GC iterative model [36]. The ambient temperature is 24 °C. Repeated charging and discharging cycles are induced to cause accelerated lithium-ion batteries aging. The capacity generated by the charge and discharge cycles is taken as a suitable health indicator to describe the degradation process of lithium-ion batteries. The experiment is terminated when the lithium-ion batteries drop below the preset FT, equal to 1.4Ahr. The capacity degradation process of four lithium-ion batteries (B0005, B0006, B0007, B0018) is shown in Fig. 10.

The GC iterative prediction model gives also the uncertainty of prediction, The B0006 lithium-ion batteries with large capacity fluctuation is selected for illustration, and we compare the linear drift term

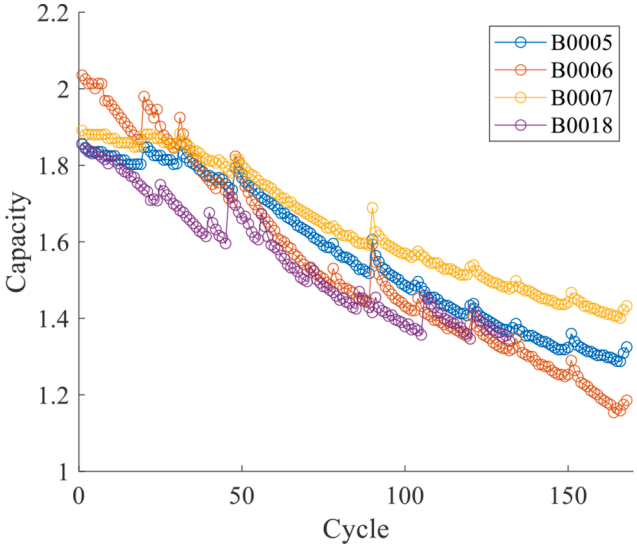

Fig. 10. Degradation process of lithium-ion batteries capacity.

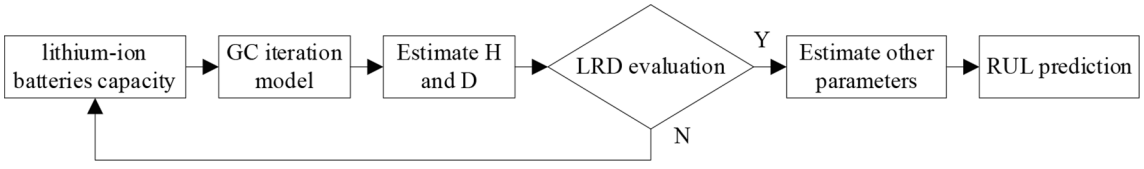

Fig. 8. Flowchart of parameter estimation procedure.

and power function drift term RUL prediction results of lithium-ion batteries. The first 50 capacity data are selected as training samples to obtain the estimated values of unknown parameters of the GC iterative model. The estimated value of the Hurst exponent H by the RS method is shown in Fig. 11: the slope of line fitting in logarithmic coordinates is the estimated value of the Hurst exponent H and is equal 0.7537. The parameters estimation results of the GC iterative model are reported in Table 1.

Then, the PDF of the RUL for 10 different prediction starting points is obtained by the Monte Carlo method, and shown in Fig. 12 at 10 different time points. The PDF of the RUL obtained by using two drift terms (M1 and M2) are both shown in Fig. 12. The blue straight line represents the actual RUL, and the five-pointed star represents the estimated value of the RUL. We obtain EOL = 109 when the B0006 lithium-ion batteries capacity exceeds FT (1.4Ahr) for the first time. The RUL estimates of M1 and M2 are reported in Table 2.

To compare the prediction accuracy, the typical indicators, mean absolute error (MAE), root mean square error (RMSE) and health degree (HD), are used. The MAE reflects the average value of the absolute error. The smaller the MAE, the more accurate the prediction:

$$MAE = \frac{1}{m}\sum_{i=1}^{m}\left|RUL_i - RUL_i^*\right| \tag{19}$$

where RUL_i is the predicted RUL obtained at the i-th prediction starting point, RUL_i^* is the actual RUL obtained at the i-th prediction starting point, $m = 10$ is the number of predictions. The RMSE describes the dispersion degree of the difference. The smaller the RMSE, the more accurate the prediction:

$$RMSE = \sqrt{\frac{1}{m}\sum_{i=1}^{m}\left(RUL_i - RUL_i^*\right)^2} \tag{20}$$

The HD is a statistic of the degree of the fitting, reflecting the degree of interpretation. The closer the HD is to 1, the closer the predicted RUL and the actual RUL are:

$$HD = 1 - \frac{\sum_{i=1}^{m}\left(RUL_i - RUL_i^*\right)^2}{\sum_{i=1}^{m}\left(RUL_i - \overline{RUL}\right)^2} \tag{21}$$

where $\overline{RUL}$ is the mean value of RUL_i.

In Table 3, the error analysis shows that the prediction accuracy of the M1 model is higher than that of the M2 model. The reason is that the linear drift term can reflect the degradation process of the lithium-ion battery capacity more accurately, which is consistent with the results in Fig. 10. Then, the comparison is made with the FBM and LSTM models

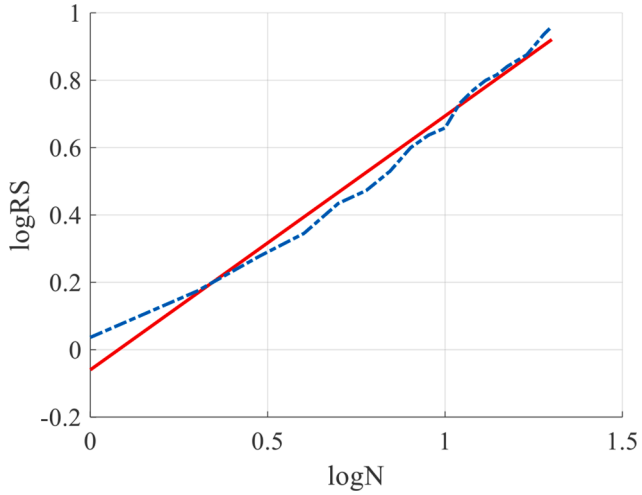

Fig. 11. RS method to estimate Hurst exponent.H

Table 1
Parameters estimation of GC iterative model.

Model	H	D	λ	σ	b
M1	0.7537	1.1606	−0.0047	0.4752	–
M2	0.7537	1.1606	−0.0060	0.4778	1.1321

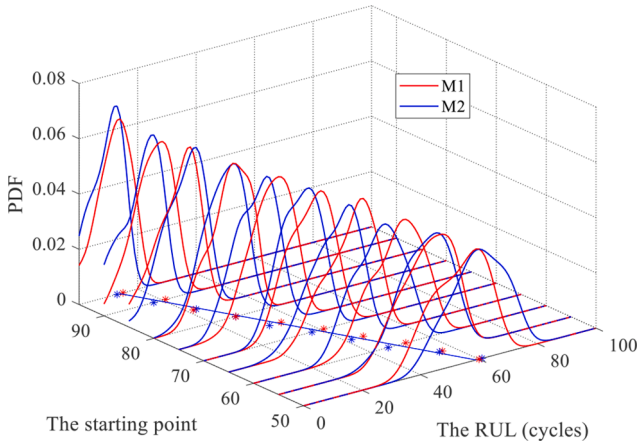

Fig. 12. Estimated PDF of the RUL by M1 and M2 for comparison.

Table 2
RUL prediction by different drift terms in the GC iterative model

Prediction starting point	Actual RUL	RUL predicted by GC (M1)	RUL predicted by GC (M2)
50	59	60	61
55	54	56	55
60	49	52	46
65	44	46	42
70	39	41	37
75	34	35	31
80	29	28	28
85	24	22	23
90	19	21	17
95	14	15	13

Table 3
Accuracy indicators of RUL prediction

Model	MAE	RMSE	HD
M1	1.7000	1.8166	0.9840
M2	1.8000	1.9494	0.9816

to verify the superiority of the GC iterative model in the accuracy of lithium-ion batteries RUL prediction. Both GC and FBM models use the linear drift term. The parameter estimation results of FBM is shown in Table 4.

The PDF comparison of lithium-ion battery RUL by using GC, FBM and LSTM models is shown in Fig. 13. The RUL estimates of the three models are given in Table 5.

The MSE, RMSE and HD are used also to compare the prediction accuracy of the different models considered. The comparison of the prediction accuracy of the GC, FBM and the LSTM models is described in Table 6.

Table 4
Parameter estimation of FBM

H	λ	σ
0.7537	−0.0042	0.4865

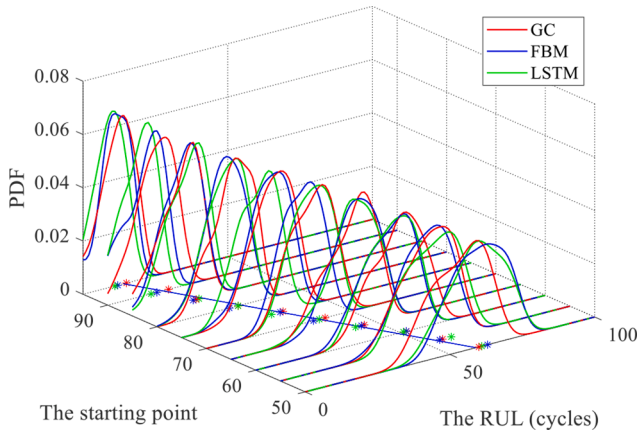

Fig. 13. Estimated PDF of the RUL by the three models used for the comparison.

Table 5
Comparison of RUL prediction of the three models

Prediction starting point	Actual RUL	RUL predicted by GC	RUL predicted by FBM	RUL predicted by LSTM
50	59	60	63	61
55	54	56	55	59
60	49	52	52	51
65	44	46	45	43
70	39	41	37	39
75	34	35	34	31
80	29	28	25	28
85	24	22	21	23
90	19	21	17	15
95	14	15	12	11

Table 6
Accuracy indicators of RUL prediction

Model	MAE	RMSE	HD
GC	1.7000	1.8166	0.9840
FBM	2.2000	2.5298	0.9690
LSTM	2.2000	2.6458	0.9661

Compared with the FBM and LSTM models, the MAE and RMSE of the GC model are lower, and the HD is close to 1. The experimental results show that the prediction accuracy of the GC iterative model is higher than FBM and LSTM models in the prediction of lithium-ion batteries RUL. The reason is that the GC iterative model with two independent parameters can describe the LRD characteristics more flexibly than the FBM with a single parameter.

5. Conclusion

This paper proposes an iterative model with LRD characteristics and applies it to predict lithium-ion batteries RUL. The specific conclusions are as follows.

(1) Accurate prediction of lithium-ion batteries RUL is of great significance to equipment safety and maintenance. In this paper, a method for predicting the lithium-ion batteries RUL using a GC iterative model is introduced. Firstly, this paper has introduced that the LRD characteristics of the GC iterative model are simultaneously described by the fractal dimension and the Hurst exponent. Therefore, the GC iterative model with two independent parameters can reflect the LRD characteristics more flexibly than the FBM with a single parameter. Then, the diffusion term is replaced by the increment of the GC time sequences to reflect uncertainty and LRD characteristics of the lithium-ion batteries capacity degradation. Finally, the comparison made with FBM and LSTM models shows that the GC iterative model has better prediction accuracy.

(2) The GC iterative model is only for the prediction of LRD time sequences: research on the short-range dependent time sequences still needs to be deepened.

CRediT authorship contribution statement

Guangxu Hong: Conceptualization, Software, Investigation, Writing – original draft. **Wanqing Song:** Validation, Methodology, Formal analysis, Visualization, Software. **Yan Gao:** Writing – review & editing. **Enrico Zio:** Writing – review & editing. **Aleksey Kudreyko:** Writing – review & editing.

Declaration of Competing Interest

The authors declare that they have no known competing financial interests or personal relationships that could have appeared to influence the work reported in this paper.

Acknowledgements

The work was supported by major project of Ministry of Science and Technology of the People's Republic of China, Grand number: 2020AAA0109301.

References

[1] R. Razavi-Far, S. Chakrabarti, M. Saif, E. Zio, An integrated imputation-prediction scheme for prognostics of battery data with missing observations, Expert Syst. Appl. 115 (2019) 709–723, https://doi.org/10.1016/j.eswa.2018.08.033.
[2] Y. Zhang, R. Xiong, H. He, M.G. Pecht, Long short-term memory recurrent neural network for remaining useful life prediction of lithium-ion batteries, IEEE Trans. Veh. Technol. 67 (7) (2018) 5695–5705, https://doi.org/10.1109/TVT.2510.1109/TVT.2018.2805189.
[3] X. Zhang, Q. Miao, Z. Liu, Remaining useful life prediction of lithium-ion battery using an improved UPF method based on MCMC, Microelectron. Reliab. 75 (2017) 288–295, https://doi.org/10.1016/j.microrel.2017.02.012.
[4] G. Jin, D.E. Matthews, Z. Zhou, A Bayesian framework for on-line degradation assessment and residual life prediction of secondary batteries inspacecraft, Reliab. Eng. Syst. Saf. 113 (1) (2013) 7–20, https://doi.org/10.1016/j.ress.2012.12.011.
[5] C. Sbarufatti, M. Corbetta, M. Giglio, F. Cadini, Adaptive prognosis of lithium-ion batteries based on the combination of particle filters and radial basis function neural networks, J. Power Sources 344 (2017) 128–140, https://doi.org/10.1016/j.jpowsour.2017.01.105.
[6] D. Wang, F.F. Yang, K.L. Tsui, Q. Zhou, S.J. Bae, Remaining useful life prediction of lithium-ion batteries based on spherical cubature particle filter, IEEE Trans. Instrum. Meas. 65 (6) (2016) 1282–1291, https://doi.org/10.1109/TIM.2016.2534258.
[7] Y. Chang, H. Fang, Y. Zhang, A new hybrid method for the prediction of the remaining useful life of a lithium-ion battery, Appl. Energy 206 (15) (2017) 1564–1578, https://doi.org/10.1016/j.apenergy.2017.09.106.
[8] X. Zheng, H. Fang, An integrated unscented kalman filter and relevance vector regression approach for lithium-ion battery remaining useful life and short-term capacity prediction, Reliab. Eng. Syst. Saf. 144 (2015) 74–82, https://doi.org/10.1016/j.ress.2015.07.013.
[9] G. Dong, Z. Chen, J. Wei, Q. Ling, Battery Health Prognosis Using Brownian Motion Modeling and Particle Filtering, IEEE Trans. Ind. Electron. 65 (11) (2018) 8646–8655, https://doi.org/10.1109/TIE.4110.1109/TIE.2018.2813964.
[10] H. Zhang, Q. Miao, X. Zhang, Z. Liu, An improved unscented particle filter approach for lithium-ion battery remaining useful life prediction, Microelectron. Reliab. 81 (2018) 288–298, https://doi.org/10.1016/j.microrel.2017.12.036.
[11] P. Duong, N. Raghavan, Heuristic Kalman optimized particle filter for remaining useful life prediction of lithium-ion battery, Microelectron. Reliab. 81 (2018) 232–243, https://doi.org/10.1016/j.microrel.2017.12.028.
[12] Z. Liu, G. Sun, S. Bu, J. Han, X. Tang, M. Pecht, Particle Learning Framework for Estimating the Remaining Useful Life of Lithium-Ion Batteries, IEEE Trans. Instrum. Meas. 66 (2) (2017) 280–293, https://doi.org/10.1109/TIM.2016.2622838.
[13] M.S.H. Lipu, M.A. Hannan, A. Hussain, M.M. Hoque, P.J. Ker, M.H.M. Saad, A. Ayob, A review of state of health and remaining useful life estimation methods for lithium-ion battery in electric vehicles: Challenges and recommendations,

J. Cleaner Prod. 205 (2018) 115–133, https://doi.org/10.1016/j.jclepro.2018.09.065.
[14] R. Khelif, B. Chebel-Morello, S. Malinowski, E. Laajili, F. Fnaiech, N. Zerhouni, Direct Remaining Useful Life Estimation Based on Support Vector Regression, IEEE Trans. Ind. Electron. 64 (3) (2017) 2276–2285, https://doi.org/10.1109/TIE.2016.2623260.
[15] X. Li, L. Zhang, Z. Wang, P. Dong, Remaining useful life prediction for lithium-ion batteries based on a hybrid model combining the long short-term memory and Elman neural networks, J. Storage Mater. 21 (2019) 510–518, https://doi.org/10.1016/j.est.2018.12.011.
[16] J.C. Chen, T.-L. Chen, W.-J. Liu, C.C. Cheng, M.-G. Li, Combining empirical mode decomposition and deep recurrent neural networks for predictive maintenance of lithium-ion battery, Measurement 50 (2021) 101405, https://doi.org/10.1016/j.aei.2021.101405.
[17] A. Nuhic, T. Terzimehic, T. Soczka-Guth, M. Buchholz, K. Dietmayer, Health diagnosis and remaining useful life prognostics of lithium-ion batteries using data-driven methods, J. Power Sources 239 (2013) 680–688, https://doi.org/10.1016/j.jpowsour.2012.11.146.
[18] X. Li, Y. Ma, J.J. Zhu, An online dual filters RUL prediction method of lithium-ion battery based on unscented particle filter and least squares support vector machine, Measurement 184 (2021), https://doi.org/10.1016/j.measurement.2021.109935.
[19] W.H. Li, Z.P. Jiao, L. Du, et al., An indirect RUL prognosis for lithium-ion battery under vibration stress using Elman neural network, Measurement 44 (2019) 12270–12276, https://doi.org/10.1016/j.ijhydene.2019.03.101.
[20] M.A. Patil, P. Tagade, K.S. Hariharan, S.M. Kolake, T. Song, T. Yeo, S. Doo, A novel multistage Support Vector Machine based approach for Li ion battery remaining useful life estimation, Appl. Energy 159 (2015) 285–297, https://doi.org/10.1016/j.apenergy.2015.08.119.
[21] Z. Zhang, X. Si, C. Hu, Y. Lei, Degradation Data Analysis and Remaining Useful Life Estimation: A Review on Wiener-Process-Based Methods, Eur. J. Oper. Res. 271 (3) (2018) 775–796, https://doi.org/10.1016/j.ejor.2018.02.033.
[22] S. Tang, C. Yu, X. Wang, X. Guo, X. Si, Remaining Useful Life Prediction of Lithium-Ion Batteries Based on the Wiener Process with Measurement Error, Energies. 7 (2) (2014) 520–547, https://doi.org/10.3390/en7020520.
[23] X. Xu, C. Yu, S. Tang, et al., Remaining Useful Life Prediction of Lithium-Ion Batteries Based on Wiener Processes with Considering the Relaxation Effect, Energies 12 (9) (2019) 1685, https://doi.org/10.3390/en12091685.
[24] H. Wang, W. Song, E. Zio, A. Kudreyko, Y. Zhang, Remaining Useful Life Prediction for Lithium-ion Batteries Using Fractional Brownian Motion and Fruit-fly Optimization Algorithm, Measurement 161 (2020) 107904, https://doi.org/10.1016/j.measurement.2020.107904.
[25] M. Li, J.Y. Li, Generalized Cauchy model of sea level fluctuations with long-range dependence, Physica A 484 (2017) 309–335, https://doi.org/10.1016/j.physa.2017.04.130.
[26] H. Liu, W.Q. Song, E. Zio, Metabolism and difference iterative forecasting model based on long-range dependent and grey for gearbox reliability, ISA Trans. (2021), https://doi.org/10.1016/j.isatra.2021.05.002.
[27] S. Lim, M. Li, A generalized Cauchy process and its application to relaxation phenomena, J. Phys. A: Math. Gen. 39 (12) (2006) 2935–2951, https://doi.org/10.1088/0305-4470/39/12/005.
[28] E. Zio, The Monte Carlo Simulation Method for System Reliability and Risk Analysis, Springer Ser. Reliab. Eng. (2013), https://doi.org/10.1007/978-1-4471-4588-2.
[29] H.e. Liu, W. Song, Y. Zhang, A. Kudreyko, Generalized Cauchy degradation model with long-range dependence and maximum Lyapunov exponent for remaining useful life, IEEE Trans. Instrum. Meas. 70 (2021) 1–12, https://doi.org/10.1109/TIM.2021.3063749.
[30] R.E. Carrillo, T.C. Aysal, K.E. Barner, A generalized Cauchy distribution framework for problems requiring robust behavior, EURASIP Journal on Advances in Signal Processing. 2010 (1) (2010) 1–19, https://doi.org/10.1155/2010/312989.
[31] S.W. Duan, W.Q. Song, E. Zio, C. Cattani, M. Li, Product technical life prediction based on multi-modes and fractional Levy stable motion, Mech. Syst. Sig. Process. 161 (12) (2021), 107974, https://doi.org/10.1016/j.ymssp.2021.107974.
[32] B. Chen, Y.G. Niu, Y.Y. Zou, Dynamic event-triggered sliding mode security control for Markovian jump systems: Learning-based iteration optimization method, Int. J. Robust Nonlinear Control (2021), https://doi.org/10.1002/rnc.5471.
[33] H. Liu, W.Q. Song, E. Zio, Generalized Cauchy difference iterative forecasting model for wind speed based on fractal time series, Nonlinear Dyn. 103 (1) (2021) 1–15, https://doi.org/10.1007/s11071-020-06150-z.
[34] J.C. Lagarias, J.A. Reeds, M.H. Wright, et al., Convergence Properties of the Nelder-Mead Simplex Method in Low Dimensions, Siam J. Optimiz. A Publication Soc. Ind. Appl. Math. 9 (1) (2006) 112–147, https://doi.org/10.1137/S1052623496303470.
[35] Y.G. Lei, N.P. Li, L. Guo, N.B. Li, T. Yan, J. Lin, Machinery health prognostics: A systematic review from data acquisition to RUL prediction, Mech. Syst. Sig. Process. 104 (2018) 799–834, https://doi.org/10.1016/j.ymssp.2017.11.016.
[36] B. Saha, K. Goebel, Battery Data Set, NASA Ames Prognostics Data Repository (2007). https://ti.arc.nasa.gov/tech/dash/groups/pcoe/prognostic-data-repository.